INNSPUB

Journal of Biodiversity and Environmental Sciences (JBES)
ISSN: 2220-6663 (Print), 2222-3045 (Online)
http://www.innspub.net
Vol. 5, No. 6, p. 407-415, 2014

RESEARCH PAPER OPEN ACCESS

Petrology and geochemistry of greenstones in Tiran area, West of Isfahan, Central Iran

Zahra Nasr-Esfahani*, Ali-Khan Nasr-Esfahani, Zahra Hossein Mirzaee

Young Researchers and Elite Club, Khorasgan (Isfahan) Branch, Islamic Azad University, Isfahan, Iran

Geology Department, Islamic Azad University, Isfahan (Khorasgan) Branch, Iran

Key words: Greenstone, Neo-Tethyan, Petrology, Sanandaj-Sirjan.

Article published on December 16, 2014

Abstract

The studied area is located in west of Isfahan province. This area is the part of Sanandaj-Sirjan structural Zone in Central Iran. This area, contain of greenschist and greenstone rocks. These rocks have metmorphed in greenschist facies and belong to the age of Triassic-Jurassic. The Greenstone is mainly composed of plagioclase, amphibole, epidote and chlorite. Geochemical data shows that parent rocks are basalt to andesitic basalt composition with sub alkaline and tholeiitic trend. These results indicated that greenstone generated volcanic environment. Greenstone in Sahrekord-Dehsard terrene shows remnants of Neo-Tethyan oceanic lithosphere with back arc basin environment that was subducted and uplifted to the surface.

***Corresponding Author:** Zahra Nasr-Esfahani ✉

Introduction

The studied area located in south Tiran in Isfahan province (Central Iran) and apart of Zagros orogen (Fig. 1). The Zagros orogen as a part of the Alpine-Himalaya mountain chain is a well-defined active doubly-vergent and asymmetric orogenic belt (Alavi, 2004) and extends in a northwest–southeast direction for about 2000km from the Taurus mountain of southeastern Turkey to the Bandar-Abas syntax in southern Iran (Arfania and Shahriari, 2009). This orogenic belt consists of four NW-SE trending parallel zones: (1) Urumieh-Dokhtar Magmatic Arc (UDMA); (2) Sanandaj-Sirjan Zone (SSZ); (3) High Zagros; and (4) Zagros Simply Folded Belt (ZSFB). The Sanandaj-Sirjan Zone (SSZ) is a narrow zone of highly deformed rocks located between the towns of Sirjan in the southeast and Sanandaj in the northwest (Mohajjel and Fergusson, 2000). The Sanandaj-Sirjan Zone is a metamorphic belt (greenschist_amphibolite facies) that was exhumed during the Cretaceous – Tertiary continental collision between the Afro-Arabian continent and the Iranian platue (e.g. Sengor and Natalin (1996), Mohajjel and Fergusson (2000); Mohajjel (2003). The rocks in this zone are the most highly deformed in the Zagros orogen and share the NW-SE trend of its structures. The Sanandaj-Sirjan Zone is thrust over the Arabian Platform along the Main Zagros Fault, which is marked at the surface by a discontinuous belt of ophiolitic rocks and mélanges running along the entire length of the orogen (Ricou, 1974). The Main Zagros Fault is deeply rooted and coincides with the suture between the Arabian Plate and Sanandaj-Sirjan Zone (Agard ., 2005, Berberian, 1995). The Zagros Fold-Thrust Belt is a result of a total shortening of 65-78km across the Zagros sedimentary basin from the Early Miocene onwards (Mouthereau ., 2007). The basin is characterized by a sequence of sedimentary rocks up to 12km thick including Paleozoic and Mesozoic shelf sediments and Cenozoic syn-orogenic strata that were deposited on the subsiding northeastern Arabian continental margin. In the Golpaygan area, the Sanandaj-Sirjan Zone can be subdivided into two parts: (i) southeastern part consisting of Jurassic metamorphosed rocks; and (ii) northwestern part, deformed in the Late Cretaceous, containing many intrusive felsic rocks (Eftekharnejad, 1981). The southeastern Sanandaj-Sirjan Zone is subdivided transversally into two separate regions: (i) northeastern region (Esfahan-Sirjan Block) consisting of Paleozoic, Mesozoic and Cenozoic sedimentary rocks with typical Central Iranian stratigraphic features and (ii) southwestern region (Shahrekord-Dehsard Terrane), which is an intensively faulted zone consisting of high to low grade metamorphic rocks and metasedimentary strata with intercalations of intermediate to basic volcanic rock. This terrane has been regarded as an old Precambrian basement (Taraz, 1974), reactivated in the course of the Mesozoic Cimmerian Orogeny (Gasemi and Hosaini, 2007). The boundary separating the southwest and the northeast regions is a major fault which Taraz (,) was the first to name as the Main Deep Fault. Study area is situated in Shahrekord–Dehsard terrain. This sub-zone is distinguished from the other sub-zones by the abundance of metamorphic rocks. These rocks metamorphed in greenschist facies and are Triassic to Jurassic age (Fig. 2). Schist, marble, amphibolite, quartzite, metadolomite, and metasandstone are the main constituents. Metamorphic conditions of these rocks are not well constrained. Earlier reports of Hercynian and older orogenies in Paleozoic rocks of the southeast complexly Deformed Sub-zone have been disputed by Alavi (1994) and most of the orogenic activity in the Sanandaj-Sirjan Zone is now related to closing of the Tethys. A large part of the Complexly Deformed Sub-zone consists of metamorphosed Mesozoic clastic, carbonate and some volcanic rocks. Subduction of Tethys under the marginal and Complexly Deformed Sub-zones has occurred to form a continental margin magmatic arc (Urumieh-Dokhtar Magmatic Arc) and associated plutonism, deformation and metamorphism (Nasr-Esfahani and Ziaei, 2007). The studied area is a large-scale ductile shear zone trending NW–SE nearly parallel to the Main Zagros Reverse.

Rocks are have undergone mylonitization causing mylonitic foliation and lineation. This area is characterized by the predominance of metamorphic rocks of both sedimentary and magmatic origins that are intruded by deformed granitoid bodies.

The metamorphic rocks are Triaaic-Jurasic age and constitute an assemblage of low grade metamorphic that have been affected by several tectono-metamorphic events (Nasr-Esfahani and Ziaei, 2007). Davoudian . (2005) reported eclogites and other metamorphed volcanic rocks in north Shahrekord, they suggest that these rocks represent relics of the Neo-Tethys oceanic plate, which was subducted under the Iranian microcontinent. This area is near north Shahrekord and geologically, the two regions are similar. In study area, metamorphic rocks are dominated by paragneisses, greenschists, greenstones, metacarbonates, which are intruded by granites (Nasr-Esfahani and Ziaei, 2007). The greenstones are important metamorphic rocks that which are assumed to be oceanic plate remains, these rocks are the focus of the present study, and may reveal important information on tectonic setting of the Sanandaj-Sirjan Zone in this area.

Materials and methods

Geological setting

The study area belongs to Shahrekord-Dehsard terrain in the north west of Isfahan and is underlain by various rocks ranging in age from Triassic to Quaternary. This area is located in 70 km NW of Isfahan, Central Iran (Fig. 1). The lower most rock units in this area constitute Triassic-Jurassic metamorphosed igneous rocks which include metabasic rocks associated with greenschist and cut by doleritic dykes (Nasr-Esfahani and Ziaei, 2007).

Jurassic sedimentary rocks consist of shale and sandstone alternation with interbedded limestone and dolomite (J1 and J2) overlie greenstones and greenschists, contact is sharp but conformable (Davoudian ., 2008). These rocks developed over the greater part of the study area. Jurassic rocks are intruded by deformed granitoid body.

This granite shows weaker metamorphic effects and they are strongly deformed during subsequent deformation events (Nasr-Esfahani and Ziaei, 2007). Cretaceous rocks are represented by marine carbonate and terrigenous-carbonate facies which rest with an angular unconformity on Jurassic underlying rocks and crop out in the north-east of area (Eliasi ., 2011).

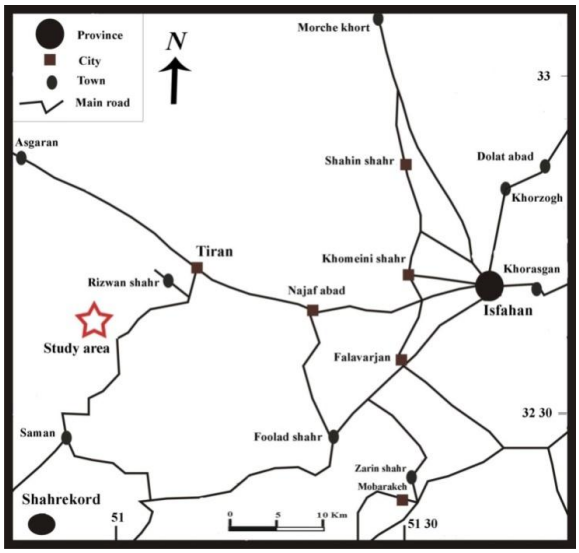

Fig. 1. Simplified geographic map of Iran.

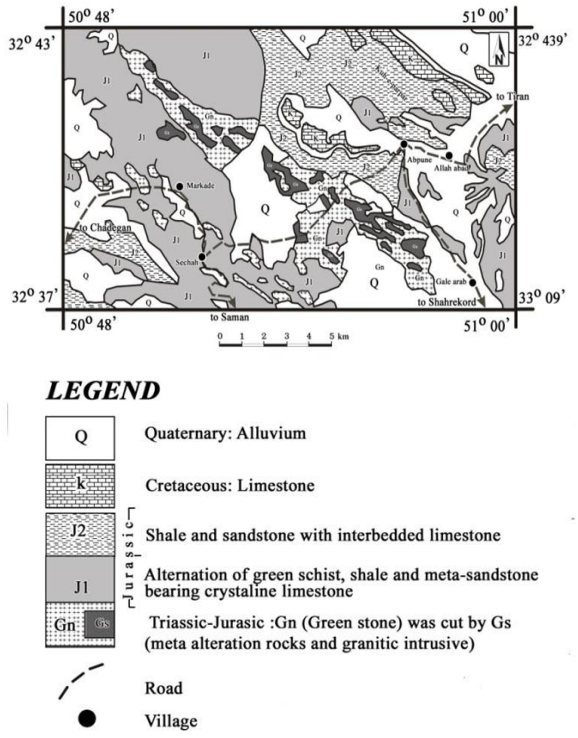

Fig. 2. Geological location of study area, modified from Gasemi and Hosaini (2007).

Sampling and Analytical techniques

A total of 68 relatively fresh samples were selected from the greenstones rocks of the study area. The samples were deformed and metamorphosed under at least greenschist facies conditions. As a result, metamorphic minerals replaced igneous minerals, and deformational fabrics are pronounced. 6 samples after microscopy study were analyzed for major, trace and rare earth elements (REE) in the ALS Chemex analytical laboratory (Vancouver, Canada) by using ICP-MS (inductively coupled plasma mass spectrometry) after acid decomposition (Table 1). Major elements were determined by ICP-MS (inductively coupled plasma atomic emission spectrometry). Major element detection limits are about 0.001-0.2%.4 samples (A.13, A.16, A.20.B, and L.20) were analyzed for major and minor elements by X-ray fluorescence spectrometry at the Laboratory of Isfahan University, Iran.

Discussion

Petrography

The meta-magmatic rocks are greenstones and dolerite dykes. They crop out south Ab-Puneh village. The meta-magmatc rocks are variably foliated. They are greenish in hand specimen due to dominance of chlorite and green amphibole (Fig. 3 and 4). They contain tremolite-actinolite, epidote, chlorite mineral paragenesis that is indicative for low-grade metamorphism. Greenstones are mainly fine to medium grained rocks, which commonly contain actinolitic amphibole, quartz, opaque minerals, and plagioclase porphyroblasts/phenocrysts (Fig. 3). Also, these minerals along with other mineral phases variably constitute the groundmass. The amphibole schist samples do not show any relict minerals and contain trace plagioclase and recrystallized quartz aggregates in the groundmass. Plagioclase with lamellar twining and amphiboles are the dominant phenocryst phases in the metabasalt and greenschist outside. In greenstone, igneous texture (ophitic/subophitic) and mineralogy (partially replaced pyroxenes, saussuritized plagioclase) are locally preserved. Also, completely replaced plagioclase and pyroxene are locally traceable in greenschists. Alterations are intense in some of the greenstone samples from shear zones. Secondary minerals include epidote, chlorite, carbonate and sericite.

Bulk sample geochemistry

Results of whole-rock geochemical analysis of all samples are presented in Table 1. The greenstone samples display SiO_2, Al_2O_3, K_2O and MgO contents ranging from 44.2 to 54.54, from 14 to 16.85, from 0.28 to 0.8 and from 2.55 to 10.55 wt% respectively. The greenstone rocks are basic to intermediate in composition with SiO_2 %wt ranging from to 44.2 to 54.54. However, most samples have SiO_2 below 51% and high MgO (>6%) indicating the predominance of modestly fractionated basalts in the series. On the base of geochemical diagrams, $Zr/TiO_2 *10^{-4}$ vs. Nb/Y diagram (Winchester and Floyd 1977, Fig. 5), the samples plot in the basalt field of this diagram. They show low Nb/Y ratio indicating subalkaline affinities (Fig.4b). This diagram is preferred to the more commonly used total-alkali-silica (TAS) classification diagram (Le Bas ., 1986) as there may have been mobility of K in some of the more altered samples. The total alkali content is low and K_2O is lower than Na_2O indicating a low-K and Fe-enriched tholeiitic nature. Tholeiitic trend is clearly indicated on the AFM diagram (Fig. 5a). Na_2O + K_2O vs. Al_2O_3 diagram (Irvine and Baragar, 1971); the greenstone is dominated by sub-alkaline tholeiitic affiliation with moderate to high-Al basalts (Fig. 5b).

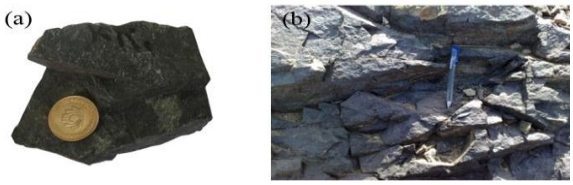

Fig. 3. Hand specimen (a) and outcrops (b) of greenstones.

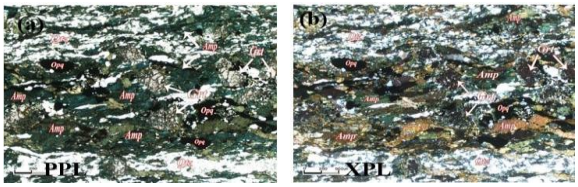

Fig. 4. Microphotograph of greenstones (Pl-plagioclase, Amp-amphibole and Opq-opaque).

Table 1. Major (Oxides: %wt) and trace elements (in ppm) data for greenstone rocks in study area.

Sample	K5	K10	K12	K12-1	K18	K20	A.13	A.16	A.20.B	L.20
SiO_2	44.2	51.7	46.7	45.4	46.2	48.5	50.091	46.78	54.54	45.071
Al_2O_3	14	15.55	14.4	14.5	16.85	14.9	10.83	15.49	14.1	14.37
Fe_2O_3T	17.7	13.15	14.35	14.95	10.3	12	11.98	10.96	7.72	10.131
CaO	9.82	7.58	10.85	10.8	9.27	9.82	10.14	10.32	4/93	9/121
MgO	6.12	2.55	6.66	6.15	10.55	6.42	6.162	3.138	9.291	8.674
Na_2O	2.3	4.41	2.64	2.43	2.16	1.64	1.603	3.223	3/069	2/267
K_2O	0.39	0.6	0.67	0.52	0.28	0.73	0.62	0.53	0/8	0/64
Cr_2O_3	0.03	0.13	0.06	0.08	0.83	0.06	....	....	....	....
TiO_2	3.69	1.8	2.23	2.32	0.78	1.5	1.26	2.069	0/637	0/984
MnO	0.25	0.18	0.27	0.26	0.18	0.21	0.206	0.135	0/084	0/146
P_2O_5	0.19	0.74	0.2	0.07	0.1	0.17	0.215	0.378	0/212	0/233
SrO	0.02	0.04	0.04	0.04	0.03	0.02	.....	.....	.....	.....
BaO	0.01	0.02	0.03	0.02	0.01	0.01	.....	.....	.....	.....
LOI	1.77	1.46	1.55	2.25	2.36	2.37	6.58	6.67	5/020	8/40
Total	100.49	99.91	100.65	99.79	99.9	98.4	99.687	99.693	100.603	99.674
Zr/Nb	8.75	31.66	6.84	17.5	18.52	17.21	13.11	9.63	12.45	19
Zr/Y	2.03	3.06	2.09	1.49	3.42	3.21	3.28	3.21	7.61	3.96
La/Nb	0.8	4.21	1.29	1.83	1.74	1.31	0.44	0.63	0.27	1
Th/Ta	0.63	6.75	2.78	1.8	2.4	2.42	.....	.....	.....	.....
Th/Yb	0.1	0.61	0.56	0.11	0.315	0.27	.....	.....	.....	.....
Ta/Yb	0.165	0.09	0.2	0.065	0.13	0.11	.....	.....	.....	.....
Nb/Y	0.23	0.096	0.31	0.85	0.185	0.186	0.25	0.33	0.61	0.21
Th/La	0.059	0.13	0.15	0.082	0.1	0.12	0.75	0.4	0.33	0
Ti/Zr	632.04	70.99	230.5	662.3	93.52	85.64	.....	.....	.....	.....
Mg#	40.9	28.07	48.11	45.16	67.17	51.61	.....	.....	.....	.....
FM	0.49	0.6	0.42	0.45	0.25	0.38	.....	.....	.....	.....
Au	<0.001	<0.001	<0.001	<0.001	<0.001	0.007				
Ag	<1	<1	<1	<1	<1	<1				
Ba	101.5	174	257	173	111.5	118.5	114	174	133	210
Co	51.3	19.7	30.5	32.7	53.1	41.9	46	28	29	42
Cr	210	900	430	570	5960	430	239	200	172	285
Cs	0.48	0.22	0.51	0.47	1.2	0.5				
Cu	48	14	21	25	69	114	91	62	5	53
Ga	19.9	26.2	20.5	18.5	15.3	18.3				
Hf	1	3.9	1.8	0.7	1.4	3				
Mo	<2	2	<2	<2	<2	<2				
Nb	4	4.8	8.6	1.2	2.7	6.1	9	8	11	5
Ni	24	11	76	33	186	51	49	9	39	157
Pb	9	10	12	11	26	20	29	46	13	15
Rb	11.1	12.3	13.1	10	7	34.7	30	18	33	28
Sn	<1	3	1	<1	1	1				
Sr	188.5	312	331	278	207	167	184	285	266	254
Ta	0.3	0.4	0.6	0.1	0.2	0.4				
Th	0.19	2.7	1.67	0.18	0.48	0.97	3	2	1	0
Tl	<0.5	<0.5	<0.5	<0.5	<0.5	<0.5				
U	0.1	0.99	0.79	0.08	0.14	0.36	4	5	9	3
V	675	129	366	417	150	288	243	229	239	143
W	3	2	3	2	2	1				
Y	17.2	49.7	27.7	14.1	14.6	32.7	36	24	18	24
Zn	161	100	176	170	294	1040	1438	605	189	289
Zr	35	152	58	21	50	105	118	77	137	95

Sample	K5	K10	K12	K12-1	K18	K20	A.13	A.16	A.20.B	L.20
Rare elements (ppm)										
La	3.2	20.2	11.1	2.2	4.7	8	4	5	3	5
Ce	7.9	46.5	23.7	5.6	10.8	18.8				
Pr	1.27	6.64	3.18	0.93	1.54	2.85				
Nd	6.9	30.5	13.8	4.9	7.2	13.4				
Sm	2.22	7.94	3.68	1.66	1.96	3.86				
Eu	1.3	2.75	1.59	1.21	0.91	1.44				
Gd	2.74	9.04	4.31	2.03	2.37	4.68				
Tb	0.53	1.56	0.81	0.42	0.43	0.93				
Dy	3.44	9.29	5.33	2.88	2.77	6.42				
Ho	0.73	1.97	1.07	0.59	0.58	1.3				
Er	2.04	5.32	3.08	1.69	1.56	3.74				
Tm	0.28	0.74	0.45	0.24	0.26	0.54				
Yb	1.81	4.41	2.96	1.53	1.52	3.6				
Lu	0.27	0.69	0.43	0.24	0.22	0.54				

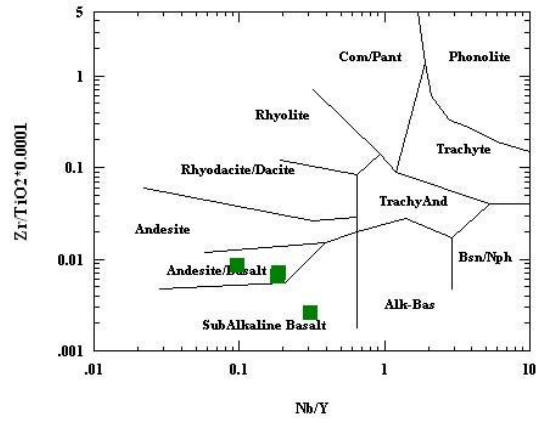

Fig. 5. Classification of magma types (a) , Zr/TiO_2 *10^{-4} vs. Nb/Y diagram (Winchester and Floyd, 1977) for greenstone.

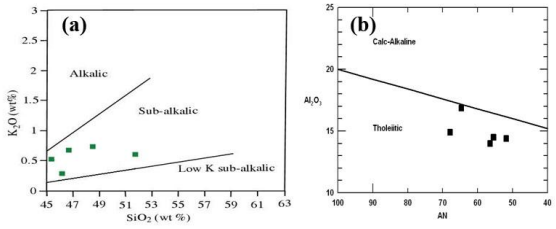

Fig. 6. The greenstone samples plot on diagrams of (a) K_2O-SiO_2 (Irvine and Baragar, 1971), (b) AN vs Al_2O_3 diagram(Kuno, 1961).

Tectonic setting

Tectonic discrimination on V-Ti/1000 [30] shows that most sample plot on the ocean floor basalt fields (Fig. 8a).

The CaO/TiO_2 and Al_2O_3/TiO_2 ratios for the basic rocks from the greenstones are shifted towards lower values than most volcanic arc rocks (Fig. 8b) suggesting a source that is not similar to the source for the modern arc lavas (Wilson, 1989) has indicated that a contribution from the subducted component in terms of the highly incompatible elements such as Ti, Zr, Y and Nb is insignificant compared to the role from the asthenospheric mantel wedge above the subducted slab. Besides, the higher ratios of the incompatible elements with respects to average basalts from oceanic island-arcs and normal mid-oceanic ridges may indicate a contribution from an incompatible elements-enriched melt.

Within-plate basalts having higher Ti/Y and higher Nb/Y reflect an enriched mantle source relative to the source of MORB and volcanic arc basalts (Rollinson, 1993), the analyzed rocks plot in the plate-margin basalts, indicating enrichment in Zr and Ti compared with Within-plate basalts (Fig. 8c). Zr/Y plotted against the fractionation index Zr (adapted from (Pearce and Norry, 1979) provided an effective discrimination between the basalts from ocean-island arcs, mid-ocean basalts, within-plate basalts and back-arc basin basalts (Rollinson, 1993), and the greenstone plot in the field of back-arc basin basalts (Fig. 8d). Back-arc basin basalts (BABB) have notably higher Zr, lower Ti/Zr, V/Ti and Sc/Y values then island arc basalts (IAB) (Woodhead . 1993).

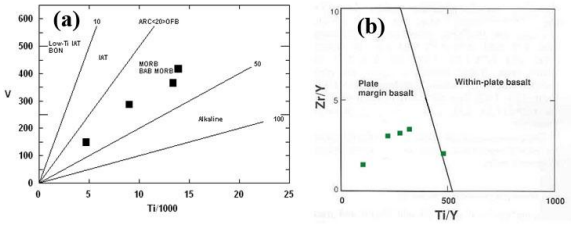

Fig. 8. Tectonic discrimination diagrams for greenstone on (a) V-Ti/1000 (Pearce and Cann, 1973), (b) Zr/Y-Ti/Y diagram (Pearce and Gale, 1977).

Conclusions

The Sanandaj-Sirjan Zone is thrust over the Arabian platform along the main Zagros Fault. The main Zagros Fault is deeply rooted and coincides with the suture between the Arabian plate and Sanandaj-Sirjan Zone. The main ambiguity on the tectonic evolution of the southeastern Zagros orogenic belt is the time when the Neo-Tethys oceanic crust disappeared completely between the central Iran microcontinent and the Arabian plate. Based on this review, the subduction of the Neo-Tethys oceanic lithosphere has continued up to middle Miocene time and final collision between the Arabian plate and the central Iran microcontinent occurred in the late micro continent. Once Neo-Tethys rifting occurred in the upper Carboniferous-lower Permian. In the upper Triassic- lower Jurassic Neo-Tethys under thrust in under central Iran microcontinent. Arfania and Shahriari have suggested that Shahrekord-Dehsard consists two oceanic basins, Neo-Tethys 1 and Neo-Tethys 2. In this model the evolution of several stages, Subduction, Oceanic lithosphere and continental collision of upper Triassic to Pliocene. During the late Triassic-early Jurassic a new spreading ridge, the second Neo-Tethys, was created to separate the Shahrekord-Dehsard terrain. From Afro- Arabian plate and developed back arc basin. Simultaneously, the second Neo-Tethys spreading and primary Neo-Tethys closing occurred in the upper Miocene and late. Probably the upper Miocene-Pleistocene, second Neo-Tethys is completely closed. According to this research, greenstones in the study area are basaltic composition with sub-alkaline and tholeiitic trend and indicated to the oceanic crust and were created in back arc basin environment. Chemically this rocks are as much enriched as N-type MORB and similar E-type MORB. Greenstone rocks are probably remnants of second Neo-Tethyan Oceanic crust with back arc basin environment. Arfania and Shahriari have showed that probably rifting and spreading jumped west to separated Shahrekord-Dehsard terrane from the north-eastern margin of the Afro-Arabian continent, creating the new Neo-Tethys (equal Neo-Tethys 2) in Trassic- Jurasic time. This new plate was probably active by the end of Mesozoic time. I suggest that because of petological and geochemical nature, greenstones represent relics of the Neo-Tethys oceanic plate, which was subducted under the Iranian microcontinent (as a part of Eurasia).

References

Agard P, Omrani J, Jolivet L, Mouthereau F. 2005. Convergence history across Zagros (Iran): Constraints from coalitional and earlier deformation. International Journal of Earth Sciences, **94**. 401–19.

Alavi M. 1994. Tectonics of the Zagros Organic belt of Iran: New Data & Interpretations Tectonophysics, **229**. 211-238.

Alavi M. 2004. Regional stratigraphy of the Zagros fold-thrust belt of Iran and its proforeland evolution. American Journal of Science. **304**. 1-20.

Arfania R, Shahriari S. 2009. Role of southeastern Sanandaj-Sirjan Zone in the tectonic evolution of Zagros Orogenic Belt, Iran. Journal of Island Arc, **18**. 555-576.

Babaie HA, Ghazi AM, Babaei A, Duncan R, Mahony J, Hassanipak A. 2003. New Ar-Ar age, isotopic, and geochemical data for basalts in the Neyriz ophiolite, Iran. Geophysical Research Abstracts **5** (12) 899.

Berberian M. 1995. Master 'blind' thrust faults hidden under the Zagros folds: Active basement tectonics and surface morphotectonics. Tectonophysics, **241**. 193–224.

Davoudian AR, Khalili M, Noorbehesht I, Mohajjel M. 2005. The tectonometamorphic & magmatic evolution in the Shahrekord- Daran area (Sanandaj-Sirjan Zone, Iran). Ph.D. thesis. University of Isfahan. 217 p.

Eftekharnejad J. 1981, Tectonic division of Iran with respect to sedimentary basins. Journal of Iranian Petroleum Society, **82**. 19–28 (in Farsi).

Fakhari MD, Axen G J, Horton B K, Hassanzadeh J, Amini A. 2008. Revised age of proximal deposits in the Zagros foreland basin and implications for Cenozoic evolution of the High Zagros. Tectonophysics, **451**, 170–85.
doi: 10.1016/j.tecto. 2007.11.064.

Floyd PA, Kelling G, Gokcen SL, Gokcen N. 1991. Geochemistry and tectonic environment of basaltic rocks from the Misis ophiolitic mélange, south Turkey. Chemical Geology, **89**. 263-80.

Gasemi A, Hosaini M. 2007. 1:100000 Geological map of Chadegan. Geological survey and mineral explorations of Iran.

Irvine TN, Baragar WRA. 1971. A guide to chemical classification of common volcanic rocks. Canadian Journal of Earth Sciences, **8.** 523-547.

Kuno H. 1961, High Alumina Basalt. Journal of petrology, **1.** 121-145.

Le Bas MJ, Le Maitre RW, Streckeisen A, Zanetin B. 1986. A chemical classification of volcanic rocks based on the total alkalies-silica diagram. Journal of Petrology, **27**. 745-750.

Le Maitre RW, Bateman P, Dudek A, Kelle J, Lameyre Le Bas M. J, Sabine PA, Schmid R, Sorensen H, Streckeisen A, Woolley AR, Zanettin B. 1989. A classification of igneous rocks and glossary of terms. Blackwell. Oxford, 193 p.

Mohajjel M, Fergusson CL, Sahandi MR. 2003. Cretaceous-Tertiary convergence and continental collision, Sanandaj-Sirjan Zone, Western Iran. Journal of Asian Earth Sciences, **21**. 397-412.

Mohajjel M, Fergusson CL. 2000. Dextral transpression in Late Cretaceous continental collision, Sanandaj - Sirjan zone, Western Iran. Journal of Structural Geology, **22** (8), 1125 - 1139.

Mouthereau F, Tensi J, Bellahsen N, Lacombe O, De Boisgollier T, Kargar S. 2007, Tertiary sequence of deformation in a thin-skinned/thick-skinned collision belt: The Zagros Folded Belt (Fars, Iran). Tectonics 26, TC5006 doi: 10.1029/ 2007TC002098.

Pearce JA, Cann JR. 1973. Tectonic setting of basic volcanic rocks determined using trace element analyses. Earth and Planetary Science Letters, **19.** 290-300.

Pearce JA, Gale GH. 1977. Identification of ore deposition environment from trace element geochemistry of associated igneous host rocks. In Volcanic Processes in Ore Genesis (Ed. M. J. Norry), Geological Society of London, 7.

Pearce JA, Norry MJ. 1979, Petrogenetic implication of Ti, Zr, Y and Nb variation in volcanic rocks. Contribution to Mineral and Petrology, 69. p. 33-47.

Reuter M, Piller WE, Harzhauser M. 2007, The Oligo-/Miocene Qom Formation (Iran): Evidence for an early Burdigalian restriction of the Tethyan Seaway and closure of its Iranian gateways. International Journal of Earth Science, 98, 627–50 doi: 10.1007/s00531-007-0269-9.

Ricou LE. 1974. L'étude géologique de la région de Neyriz (Zagros iranien) etl'évolution des Zagrides. Thesis, Université Paris-Sud, Orsay.

Rollinson H. 1993, Using geochemical data: evaluation, presentation, interpretation. Longman Scientific and Technical., 352 p.

Sengor M.C, Natalin BA. 1996. Paleotectonics of Asia: Fragments of a synthesis. In Yin A. & Harrison T. M. (eds.) The Tectonic Evolution of Asia, p. 486–640, Cambridge University Press, Cambridge.

Shafaii-Moghadam H, Rahgoshay M, Whitechurch H. 2007. The Naien-Baft ophiolites: An evidence of back-arc basin spreading in the active margin of the Iranian continent. Geophysical Research Abstracts, **9.** 791 p.

Shahabpour J. 2007. Island-arc affinity of the Central Iranian Volcanic Belt. Journal of Asian Earth Sciences, **30.** 652–65

Sun SS, McDonough WF. 1989. chemical and isotopic systematic of oceanic basalts: implication for mantle composition and processes. In: Sunders, A.D.,Norry, M.J.(Eds.), Magmatic in Oceanic Basins, Special Publication. 42.Geology Society of London, 313–345.

Sun SS, Nesbitt RW. 1978, Geochemical regularities and genetic significance of ophiolitic basalts. Geology **6.** 689-693.

Taraz H. 1974. Geology of the Surmagh-Deh Bid Area, Abadeh Region, Central Iran. Report (37). Geological Survey of Iran, Tehran.

Taylor SR, McLennan SM. 1985. the Continental Crust: its Composition and Evolution. Blackwell, Cambridge. 312 p.

Wilson M. 1989. Igneous petrogenesis. Unwin Hyman, London, 1- 46

Winchester JA, Floyd PA. 1977. Geochemical discrimination of different magma series and their differentiation products using immobile elements. Chemical of Geology, **20.** 325-343.

Woodhead J, Eggins S, Gamble J. 1993. High field strength and transition element system in island arc back-arc basin basalts: evidence for multi-phase melt extraction and depleted mantle wedge. Earth and Planetary Science Letters, **114.** 491-504.